

TYPE I PLANET MIGRATION IN NEARLY LAMINAR DISKS

H. Li¹, S. H. Lubow², S. Li¹, D.N.C. Lin³

ABSTRACT

We describe 2D hydrodynamic simulations of the migration of low-mass planets ($\leq 30M_{\oplus}$) in nearly laminar disks (viscosity parameter $\alpha < 10^{-3}$) over timescales of several thousand orbit periods. We consider disk masses of 1, 2, and 5 times the minimum mass solar nebula, disk thickness parameters of $H/r = 0.035$ and 0.05 , and a variety of α values and planet masses. Disk self-gravity is fully included. Previous analytic work has suggested that Type I planet migration can be halted in disks of sufficiently low turbulent viscosity, for $\alpha \sim 10^{-4}$. The halting is due to a feedback effect of breaking density waves that results in a slight mass redistribution and consequently an increased outward torque contribution. The simulations confirm the existence of a critical mass ($M_{cr} \sim 10M_{\oplus}$) beyond which migration halts in nearly laminar disks. For $\alpha \gtrsim 10^{-3}$, density feedback effects are washed out and Type I migration persists. The critical masses are in good agreement with the analytic model of Rafikov (2002). In addition, for $\alpha \lesssim 10^{-4}$ steep density gradients produce a vortex instability, resulting in a small time-varying eccentricity in the planet's orbit and a slight outward migration. Migration in nearly laminar disks may be sufficiently slow to reconcile the timescales of migration theory with those of giant planet formation in the core accretion model.

Subject headings: accretion, accretion disks — hydrodynamics — methods: numerical — planetary systems: formation — planetary systems: protoplanetary disks — solar system: formation

1. Introduction

The standard theory of Type I (low planet mass) migration presents a challenge for understanding planet formation. According to the core accretion model, the growth time

¹Los Alamos National Laboratory, Los Alamos, NM 87545; hli@lanl.gov; sli@lanl.gov

²Space Telescope Science Institute, 3700 San Martin Drive, Baltimore, MD 21218; lubow@stsci.edu

³UCO/Lick Observatory, University of California, Santa Cruz, CA 95064; lin@ucolick.org

from planetesimals to gas giant planets is dominated by a phase that occurs when a newly formed solid core with mass $\sim 10M_{\oplus}$ accretes gas (Pollack et al 1996, Hubickyj et al 2007). The duration of this slow phase, $\sim 10^6y$, is determined by a thermal bottleneck that prevents the gaseous envelope from contracting, until it achieves sufficient mass. On the other hand, the standard theory of Type I migration (Tanaka et al 2002) predicts that planets in the slow growth phase would migrate into the disk center in $\sim 10^5y$ for the minimum solar mass nebula. These migration timescales have been confirmed by multidimensional hydrodynamical simulations (Bate et al 2003, D’Angelo & Lubow 2008). Recently, Ida & Lin (2008) and Schlaufman, Lin, & Ida (2008) have studied the effect of the ice line on the disk surface density profile and consequently on the Type I migration. They obtained much better agreement with the observed extrasolar planet mass-semimajor axis distribution if the Type I migration is reduced by an order-of-magnitude from the linear theory values.

The shortness of the standard migration timescale has motivated investigations of possible effects to slow or even reverse migration. These include magnetic fields (Terquem 2003), magneto-rotational instability (MRI) turbulent fluctuations (Nelson & Papaloizou 2004), and density traps (Menou & Goodman 2004). Recently, protoplanet migration in the non-isothermal disks has been investigated (Paardekooper & Mellema 2006; Baruteau & Masset 2008; Paardekooper & Papaloizou 2008; Kley & Crida 2008). These simulations show indications of slowing migration due to coorbital torques for certain ranges of gas diffusivity and turbulent viscosity. In this Letter we discuss another mechanism that naturally occurs when the disk turbulent viscosity is sufficiently small.

The Tanaka et al (2002) Type I migration rates were derived under the assumption that the disk density distribution is unaffected by the presence of the planet. Numerical simulations commonly adopt turbulent viscosity parameter values $\alpha \gtrsim 10^{-3}$. Such values are suggested by considering the observationally inferred disk masses and accretion rates for T Tauri stars (e.g., Hartmann et al 1998). With such α values, turbulent diffusion suppresses disk disturbances for planets of mass less than $0.1M_J$. The numerical simulations then satisfy the Tanaka et al (2002) assumptions and yield migration rates that are in close agreement.

The various models of planet formation by core accretion typically involve lower α values, $\alpha < 10^{-3}$ (see Cuzzi & Weidenschilling 2006), which we refer to as nearly laminar values. To form planetesimals via gravitational instability from small dust particles (Safronov 1969, Goldreich & Ward 1973) requires the dust layer to be very thin $\sim 10^{-4}H$, suggesting $\alpha \ll 10^{-4}$. For the solids to be dynamically decoupled from the gas requires a dust layer disk of thickness $\lesssim 10^{-2}H$, again suggesting nearly laminar conditions. Cuzzi & Weidenschilling (2006) estimate that $\alpha \lesssim 2 \times 10^{-4}$ in order that meter size solids avoid destructive effects of collisions due to turbulent motions.

In the planet formation regions of disks, considerations of the MRI (Balbus & Hawley 1991) suggest that the disk maybe unstable only in surface layers, due to the low levels of ionization below these layers (Gammie 1996). A major uncertainty is the abundance of small grains that can suppress the instability. The disk may be nearly laminar for the purposes of planet formation. However, surface layer turbulent fluctuations may propagate disturbances to the disk midplane. They may provide some effective turbulence in that region as well (Fleming & Stone 2003; Turner & Sano 2008).

In nearly laminar disks, density waves launched by a planet at various Lindblad resonances can redistribute disk mass as they damp. The disk turbulent viscosity needs to be sufficiently small for the density perturbation to not diffuse away. The redistributed gas slightly enhances (reduces) the disk density interior (exterior) to the orbit of an inwardly migrating planet. Some analytic studies have shown that such density feedback effects could slow and even halt the migration (Hourigan & Ward 1984; Ward & Hourigan 1989; Ward 1997; Rafikov 2002). The critical planet mass at which the feedback becomes important depends on the efficiency of the damping of waves excited by the planet. Wave damping may be due to the shock dissipation and will generally occur nonlocally, at some distance from the radius where the wave is launched. In this *Letter*, we explore the consequences of nearly laminar disks on planet migration by means of nonlinear 2D numerical simulations.

2. Numerical Method and Initial Setup

We assume that the protoplanetary disk is thin and can be described by the 2D isothermal Navier-Stokes equations in a cylindrical $\{r, \phi\}$ plane centered on the star with vertically integrated quantities. The differential equations are the same as given in Kley (1999). Simulations are carried out using a hydro code developed at Los Alamos (Li et al. 2005). We also use the local comoving angular sweep as proposed in the FARGO scheme of Masset (2000) and modified in Li et al. (2001). The equations of motion of the planets are the same as given in D’Angelo et al. (2005), which we adapted to the polar coordinates with a fourth-order Runge-Kutta solver. During each hydrodynamics time step, the motion of the planet is divided into several substeps so that the planet always moves within 0.05 local grid spacing, $\delta = [(\Delta r)^2 + (r_i \Delta \phi)^2]^{1/2}$, in one substep. The disk gravitational force on the planet is assumed to evolve linearly with time between two hydrodynamics time steps. Furthermore, we have implemented a full 2D self-gravity solver on our uniform disk grid (Li, Buoni, & Li 2008). This solver uses a mode cut-off strategy and combines FFT in the azimuthal direction and direct summation in the radial direction. The algorithm is sufficiently fast that the self-gravity solver costs less than 10% of the total computation cost in each run. This

code has been extensively tested on a number of problems. With our pseudo-3D treatment (see Li et al. 2005 for details) and a small (a few grid size) softening distance in the planet’s potential, migration rates from simulations with sufficient viscosity (dimensionless kinematic viscosity $\nu \simeq 10^{-6}$) agree well (within a few percent) with the 3D linear theory results by Tanaka et al. (2002). As the softening distance increases to r_H , the migration rates from such simulations are $\sim 30\%$ slower than the 3D linear theory result. The runs presented here use r_H as the softening distance.

The 2-D disk is modeled between $0.4 \leq r \leq 2$. The planet is initially located at $r = 1$, which corresponds to a physical distance of Jupiter’s orbital radius (5.2 AU), and orbits about a $1M_\odot$ star. The unit of time is the initial orbit period P of the planet, which is about 12 yr. A corotating frame that rotates with the initial angular velocity of the planet is used. The coordinate plane is centered on the central star at $(r, \phi) = (0, 0)$ (acceleration due to frame rotation is also included, the so-called indirect term). The disk is assumed to be isothermal throughout the simulated region, having a constant sound speed c_s . The dimensionless disk thickness is scaled by the initial orbital radius of the planet $h = c_s/v_\phi(r = 1)$, where v_ϕ is the Keplerian velocity. We consider values $h = 0.035$ or 0.05 in the simulations. We have also made runs using constant disk aspect ratio H/r , and found that our main conclusions are not changed.

Our numerical schemes require two ghost cells in the radial direction (the angular direction is periodic). Holding these ghost cells at the initial steady state values produced the weakest boundary reflections among all boundary conditions we investigated. We choose an initial surface density profile normalized to the minimum mass solar nebular model (Hayashi 1981) as $\Sigma(r) = 152 f(r/5\text{AU})^{-3/2} \text{ gm cm}^{-2}$, where f ranges from 1 – 5 in our simulations. The initial rotational profile of the disk is calculated so that the disk will be in equilibrium with the disk self-gravity and pressure (without the planet). The mass ratio between the planet and the central star is $\mu = M_p/M_*$, which ranges from 3×10^{-6} to 10^{-4} . The planet’s Hill (Roche) radius is $r_H = r_p(\mu/3)^{1/3}$. The dimensionless kinematic viscosity ν (normalized by $\Omega^2 r$ at the planet’s initial orbital radius) is taken to be spatially constant and ranges between 0 and 10^{-5} . For $h = 0.05$, the effective Shakura and Sunyaev $\alpha = \nu/h^2$ at the initial planet radius ranges between 0 and 4×10^{-3} . We have performed various tests to show that when $\nu = 0$, the effective numerical viscosity in our simulations is $\nu < 10^{-9}$ or $\alpha < 4 \times 10^{-7}$. We typically evolve the disk without the planet for $10 P$. Subsequently, the planet’s gravitational potential is gradually “turned-on” over a 30-orbit period, allowing the disk to respond to the planet potential gradually. Note that the time shown in all the figures in this *Letter* starts at the time of the planet release. Runs are made typically using a radial and azimuthal grid of $(n_r \times n_\phi) = 800 \times 3200$, though we have used higher resolution to ensure convergence on some runs. Simulations typically last several thousand orbit periods

at $r = 1$.

3. Results

Figure 1 shows the influence of the imposed disk viscosity on the migration for a planet with $\mu = 3 \times 10^{-5}$ or $10M_{\oplus}$, $h = 0.035$, and $f = 5$. For relatively large viscosity ($\nu = 10^{-6}$, $\alpha = 8 \times 10^{-4}$), the migration rates agree well with the Type I rates given by Tanaka et al. (2002), as discussed above. At early times the migration rates are largely independent of the disk viscosity. As viscosity decreases, after about $100 P$, the migration is drastically slowed or completely halted. The rapid oscillations with modest amplitude at $t \sim 800P$ are due to the excitation of vortices from a secondary instability (Koller et al. 2003; Li et al. 2005; see also Li et al. 2001), which will be a subject for future studies. Figure 2 reveals the reason for the slow-down. A partial gap in the disk around the planet has formed at $t = 500P$ and the density profile deviates significantly from the initial power-law. The asymmetry in the density distribution interior and exterior to the planet has reduced the contribution from the outer Lindblad torque so that the net torque is approximately zero. We verified that the slow-down shown in Fig. 1 is largely caused by the density redistribution. In principle, the torque distributions per unit disk mass ($dT/dM(r)$ see Fig 1 in D’Angelo & Lubow 2008) could also be affected. But we find these changes only slightly modify (at the few percent level) the net migration torque.

In the case of $\nu = 10^{-6}$ in Fig 2, the profile is qualitatively similar to the expectations of steady state theory (Ward 1997; Rafikov 2002). In particular there is a density peak at $r < r_p$ and a trough at $r > r_p$. The torque that the disk exerts on the planet is localized to a region of a few times the disk thickness or about $\pm 4r_H$ from radius r_p . In Fig 2 for $\nu = 10^{-6}$, we see that the perturbed density extends over a somewhat greater region of space, suggesting that nonlocal damping is involved.

In the case of lower viscosities, $\nu = 10^{-7}, 10^{-9}$ in Fig 2, the density profiles are quite different from the $\nu = 10^{-6}$ case. In these cases, the planet has effectively stopped migrating and the planet is opening a gap. We find that the gap deepens over time, i.e., the system does not reach a steady state. The large density gradients cause the vortex instability to develop, as discussed above.

The strong density feedback in nearly inviscid disks and the reduction in the total torque suggest the existence of critical planet mass above which migration can be slowed significantly or halted. Fig. 3 shows the transition from the usual Type I migration to a much slower migration as the planet mass is increased, for $f = 2$, $h = 0.035, 0.05$, and

$\nu = 0$. The reduction in migration rates is gradual, so it is difficult to define a single value above which the migration will be halted. The values we determine apply over the time range of several thousand P . We have performed a large number of runs for six different disk properties: $f = 1, 2, 5$, $h = 0.035$ and 0.05 . In Table 1 we give the estimates of the planet masses in which the migration has significantly slowed in our simulations. Above these values, migration was found to be halted.

Previous studies have emphasized the role of gap formation in slowing down the planet migration (Lin & Papaloizou 1986; Crida & Morbidelli 2007). From Fig. 2, we can see that a partial gap is formed at late time. But the slowing down of the migration has started much earlier (see also Fig. 3) where the gap is much less deep. This is consistent with our interpretation that the slowing down of the migration is primarily caused by the torque resulting from the asymmetric mass re-distribution, i.e., the density feedback effects discussed at the end of §1. With the planet mass above the critical mass, it is no longer possible to have steady state migration (as explained in the analytic studies). In this regime, a gap gradually develops and it deepens with time. But, it is still the asymmetry in the density distribution (see Fig. 2) that ensures a much reduced (or zero) net total torque.

4. Discussions

The local wave damping model of Ward & Hourigan (1989) suggests critical planet masses of $M_{cr} \sim \Sigma r_p^2 h^3$, which evaluates to $0.006fM_\oplus$ and $0.02fM_\oplus$ for $h = 0.035$ and 0.05 , respectively. These values differ from Table 1 by a factor of more than 100. However the scaling of the critical mass with disk thickness is close to h^3 as given by this theory. The scaling of M_{cr} with surface density in Table 1 is, however, weaker than that suggested by this theory. In another local wave damping model, Ward (1997) suggests that $M_{cr} \sim 0.2\Sigma r_p^2 h$, which evaluates to $1.1fM_\oplus$ and $1.6fM_\oplus$ for $h = 0.035$ and 0.05 , respectively. Although these values are numerically closer to the simulation values in Table 1, the predicted linear scaling in both f and h does not agree with the trends in the Table 1. The analytic model of Rafikov (2002) includes the effects of nonlocal damping by means of shocks. In that case, the critical masses are given by

$$M_{cr} = \frac{2c_s^3}{3\Omega G} \min [5.2Q^{-5/7}, 3.8(Q/h)^{-5/13}], \quad (1)$$

where $Q = \Omega c_s / (\pi G \Sigma)$. All the simulated cases correspond to the strong feedback branch of M_{cr} that is given by the second argument of the *min* function. Values for these critical masses are also given in Table 1. We see that the agreement between the simulation and theory is quite good.

The critical masses are in the range of the core masses during the slow phase of gas accretion in the core accretion model of planet formation. This result suggests that planet migration might not be a limiting factor in planet formation. The phase of run-away mass accretion follows the slow evolution phase. Previous studies suggest that run-away mass accretion to $1M_J$ in a disk with $\alpha \simeq 0.004$ occurs in about $10^5 y$ (e.g., D’Angelo & Lubow 2008). During this phase, we speculate that more modest levels of turbulent viscosity $10^{-4} < \alpha < 10^{-3}$ may provide sufficient accretion to form a $1M_J$ planet within $\sim 10^6 y$, while remaining in this nearly laminar disk regime of slow Type I migration.

Although this picture is suggestive of a resolution of the migration problem, the longer term evolution of nearly laminar disk-planet systems requires further exploration. The slowly migrating planet will continue to create a deeper gap over time. The steepening density gradients should lead to the vortex instability (Koller et al. 2003; Li et al. 2005). The consequences of the vortex instability should be explored.

The research at LANL is supported by a Laboratory Directed Research and Development program. S.L. acknowledges support from NASA Origins grant NNX07AI72G.

REFERENCES

- Balbus, S. A., & Hawley, J. F. 1991, *ApJ*, 376, 214
- Baruteau, C., & Masset, F. 2008, *ApJ*, 672, 1054
- Bate, M. R., Lubow, S. H., Ogilvie, G. I., & Miller, K. A. 2003, *MNRAS*, 341, 213
- Crida, A., & Morbidelli, A. 2007, *MNRAS*, 377, 1324
- Cuzzi, J. N., & Weidenschilling, S. J. 2006, *Meteorites and the Early Solar System II*, 353
- D’Angelo, G., Bate, M. R., & Lubow, S. H. 2005, *MNRAS*, 358, 316
- D’Angelo, G., & Lubow, S. H. 2008, *ApJ*, 685, 560
- Fleming, T., & Stone, J. M. 2003, *ApJ*, 585, 908
- Gammie, C. F. 1996, *ApJ*, 457, 355
- Goldreich, P., & Ward, W. R. 1973, *ApJ*, 183, 1051
- Hartmann, L., Calvet, N., Gullbring, E., & D’Alessio, P. 1998, *ApJ*, 495, 385

- Hayashi, C. 1981, Progress of Theoretical Physics Supplement, 70, 35
- Hourigan, K., & Ward, W. R. 1984, Icarus, 60, 29
- Hubickyj, O., Bodenheimer, P., & Lissauer, J. J. 2005, Icarus, 179, 415
- Ida, S., & Lin, D. N. C. 2008, ApJ, 685, 584
- Kley, W. 1999, MNRAS, 303, 696
- Kley, W., & Crida, A. 2008, A&A, 487, L9
- Koller, J., Li, H., & Lin, D. N. C. 2003, ApJ, 596, L91
- Li, H., Colgate, S. A., Wendroff, B., & Liska, R. 2001, ApJ, 551, 874
- Li, H., et al. 2005, ApJ, 624, 1003
- Li, S., Buoni, M. J., & Li, H. 2009, ApJS, in press
- Lin, D. N. C., & Papaloizou, J. 1986, ApJ, 309, 846
- Masset, F. 2000, A&AS, 141, 165
- Menou, K., & Goodman, J. 2004, ApJ, 606, 520
- Nelson, R. P., & Papaloizou, J. C. B. 2004, MNRAS, 350, 849
- Paardekooper, S.-J., & Mellema, G. 2006, A&A, 459, L17
- Paardekooper, S.-J., & Papaloizou, J. C. B. 2008, A&A, 485, 877
- Pollack, J. B., Hubickyj, O., Bodenheimer, P., Lissauer, J. J., Podolak, M., & Greenzweig, Y. 1996, Icarus, 124, 62
- Rafikov, R. R. 2002, ApJ, 572, 566
- Safronov, V. S. 1969, *Evoliutsiia Doplanetnogo Oblaka* (Moscow: Izdate;’stvo Nauka)
- Schlaufman, K. C., Lin, D. N. C., & Ida, S. 2009, ApJ, in press
- Tanaka, H., Takeuchi, T., & Ward, W. R. 2002, ApJ, 565, 1257
- Terquem, C. E. J. M. L. J. 2003, MNRAS, 341, 1157
- Turner, N. J., & Sano, T. 2008, ApJ, 679, L131

Ward, W. R. 1997, *Icarus*, 126, 261

Ward, W. R., & Hourigan, K. 1989, *ApJ*, 347, 490

Table 1: Critical Planet Mass $M_{cr}(M_{\oplus})$ from Simulations and Theory (Rafikov 2002)

	$f = 1$		$f = 2$		$f = 5$	
h	simulation	theory	simulation	theory	simulation	theory
0.05	~ 9	8.4	~ 9	10.9	~ 15	15.5
0.035	~ 3	2.9	~ 3	3.7	~ 6	5.3

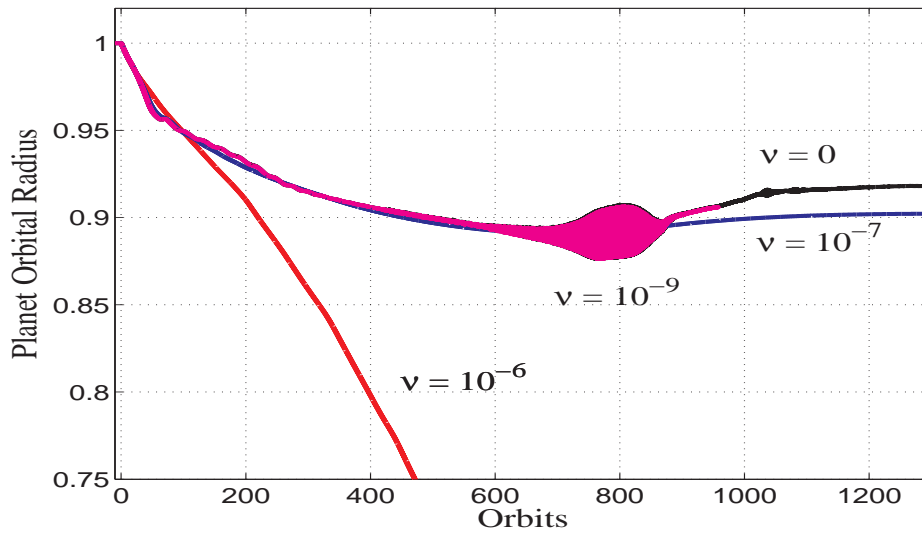


Fig. 1.— Influence of dimensionless disk viscosity ν on the migration of a planet with mass $10M_{\oplus}$ in a disk with $h = 0.035$ and $f = 5$. The vertical axis is the orbital radius in units of the initial orbital radius. The horizontal axis is the time in units of the initial planet orbital period, P . For dimensionless kinematic viscosity $\nu = 10^{-6}$ ($\alpha = 8 \times 10^{-4}$), the planet undergoes the typical Type I migration, but its migration is slowed significantly when ν is smaller.

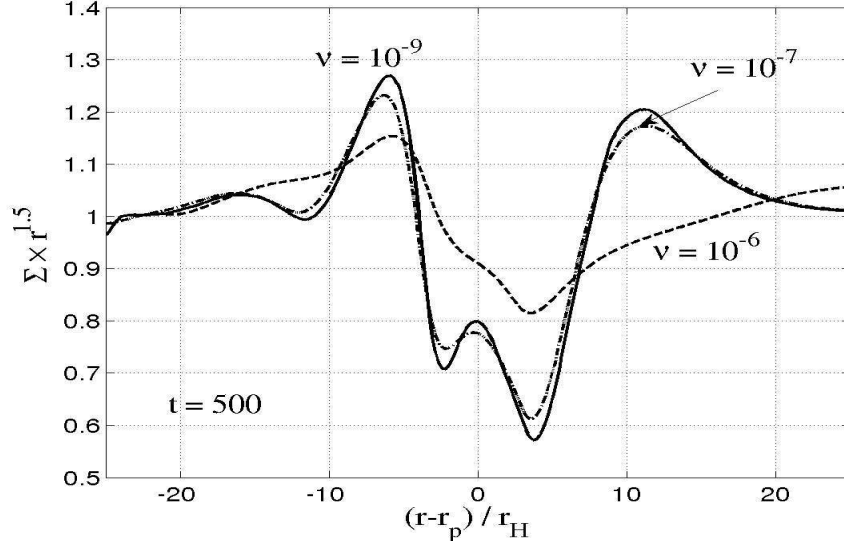


Fig. 2.— Azimuthally averaged disk surface density distribution ($\Sigma \times r^{1.5}$), normalized by its initial value at the orbital radius of the planet, at time $t = 500P$. The horizontal axis is the radius relative to the planet radius in units of the Hill radius. Model parameters are the same as in Fig. 1. The initial $\Sigma \times r^{1.5}$ is constant and equal to unity. For the lower viscosities, a gap is opening.

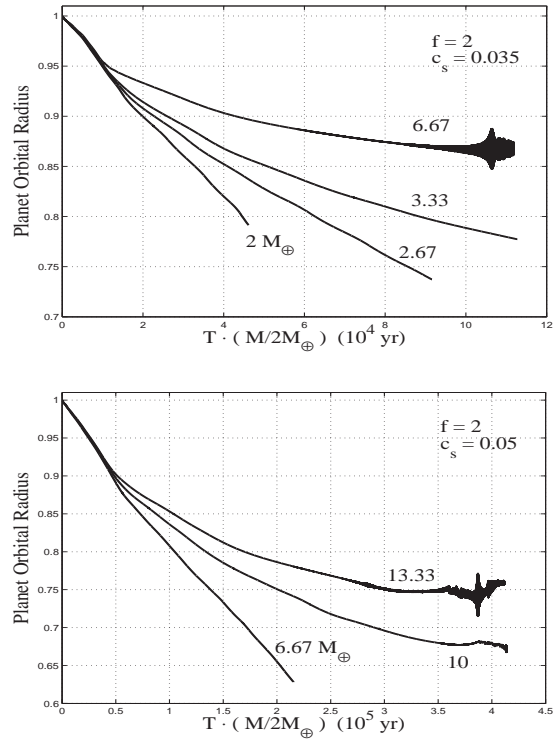


Fig. 3.— Migration history for several planet masses in nearly inviscid ($\nu = 0$) disks. As the planet mass increases, its migration transitions from the Type I to being much slower. The vertical axis is the planet orbital radius in units of the initial orbital radius. The horizontal axis is the time multiplied by the ratio of the planet mass to $2M_{\oplus}$. Each planet is assumed to have an initial orbital period of 11.87 yr.